

**Strongly nonlinear waves in capillary electrophoresis**

Zhen Chen and Sandip Ghosal\*

*Department of Mechanical Engineering, Northwestern University, Evanston, Illinois 60208, USA*

(Received 23 September 2011; revised manuscript received 30 January 2012; published 25 May 2012)

In capillary electrophoresis, sample ions migrate along a microcapillary filled with a background electrolyte under the influence of an applied electric field. If the sample concentration is sufficiently high, the electrical conductivity in the sample zone could differ significantly from the background. Under such conditions, the local migration velocity of sample ions becomes concentration-dependent, resulting in a nonlinear wave that exhibits shocklike features. If the nonlinearity is weak, the sample concentration profile, under certain simplifying assumptions, can be shown to obey Burgers' equation [Ghosal and Chen, *Bull. Math. Biol.* **72**, 2047 (2010)], which has an exact analytical solution for arbitrary initial condition. In this paper, we use a numerical method to study the problem in the more general case where the sample concentration is not small in comparison to the concentration of background ions. In the case of low concentrations, the numerical results agree with the weakly nonlinear theory presented earlier, but at high concentrations, the wave evolves in a way that is qualitatively different.

DOI: [10.1103/PhysRevE.85.051918](https://doi.org/10.1103/PhysRevE.85.051918)

PACS number(s): 87.10.-e, 87.85.mg, 87.85.dh

**I. INTRODUCTION**

In capillary electrophoresis (CE), separation of charged molecular species is accomplished by exploiting the differential migration of ions in a narrow channel (10–100  $\mu\text{m}$ ) in which a strong electric field ( $\sim 100$  V/m) is applied in the axial direction [1,2]. The sample ions exist in solution in an electrolytic buffer which is referred to as the background electrolyte (BGE). Separation is accompanied by the competing process of diffusive spreading in the axial direction, which causes peak dispersion. Dispersion reduces resolution of the separation and may lower the peak concentration to below the detection threshold. It is therefore detrimental. Any effect that tends to increase axial spreading over the minimum imposed purely by molecular diffusion in the axial direction is referred to as “anomalous dispersion” [3]. The transport problem of ions in the capillary is of considerable interest as it determines the amount of dispersion of the sample peak.

In this paper, we are concerned with an effect known as “electromigration dispersion” (EMD) that causes significant anomalous dispersion when the ratio of sample to background ion concentration becomes large enough. For this reason, it is also known as the “sample overloading effect.” In CE, it is desirable to have the sample concentration at the inlet as high as possible (to ensure that even trace components are within detectable limits) and buffer conductivity as low as possible (to minimize Joule heat), so that the limitation imposed by EMD quickly becomes significant [4].

The physical mechanism of EMD may be explained roughly in the following way: when the concentration of sample ions is sufficiently high in comparison to that of the background electrolyte, the local electrical conductivity of the solution is altered in the region around the sample peak. However, charge conservation requires the electric current to be the same at all points along the axis of the capillary. If diffusion currents due to concentration inhomogeneities are ignored for the moment, it follows that the electric field must change axially. This is

because Ohm's law, taken together with current conservation, implies that the product of the conductivity and electric field must remain constant along the capillary. The axially varying electric field then alters the effective migration speed of the sample ions, which in turn alters its concentration distribution. Thus, in the continuum limit, the concentration of sample ions is described by a nonlinear transport equation. As expected, the CE signal exhibits features reminiscent of nonlinear waves familiar from other physical contexts [5,6].

A one-dimensional nonlinear hyperbolic equation for the sample ion concentration may be derived using simplifications that arise from assuming local electroneutrality and from neglecting the diffusivity of ions [7]. The restriction to zero ionic diffusivities was recently removed by Ghosal and Chen [5]. They considered the minimal model of a three-ion system—the sample ion, a co-ion, and a counter-ion. The diffusivities of the three ionic species were assumed equal, though not necessarily zero. The sample ion concentration was then shown to obey a one-dimensional nonlinear advection-diffusion equation which reduced to Burgers' equation if the sample concentration was not too high relative to that of the background ions.

In this paper, we focus on the minimal three-ion system considered by Ghosal and Chen [5], but we do not assume that the concentration of sample ions is small. Local electroneutrality is, however, an excellent approximation in CE systems, since characteristic length scales are much larger than the Debye length, which is on the order of nanometers. We therefore exploit it to reduce the numerical stiffness of the coupled ion transport equations. We identify a small number of parameters that primarily determine the system evolution and study the dynamics for a representative range of these parameters. We show that at low concentrations, the peak evolves in accordance with the weakly nonlinear theory [5], but at high enough concentrations, the dynamics of peak evolution is qualitatively different as the system is dominated by the nonlinearity. Surprisingly, in the strongly nonlinear regime, the peak breaks up into two zones marked by a critical concentration ( $\phi = \phi_c$ ) and separated by a diffusive boundary. The high concentration zone ( $\phi > \phi_c$ ) remains quasistationary

\*s-ghosal@northwestern.edu

whereas the low concentration zone propagates forward forming a “surge front” superficially resembling nonlinear wave phenomena familiar in the context of water waves, such as a river bore [8]. The critical concentration ( $\phi_c$ ) can be predicted by a simple argument based on flux conservation. At late times, dispersion ensures that concentrations throughout the domain get smaller and the peak once again may be described by Burgers’ equation. The complex nonlinear behavior is a consequence of the nonlinearity inherent in the Nernst-Planck equations of ion transport, just as the behavior of large-amplitude water waves arises from the nonlinear nature of the Navier-Stokes equations of hydrodynamics.

## II. NUMERICAL SIMULATIONS

We set up and solve numerically an idealized problem in which a sample peak migrates in a background electrolyte. The channel walls are assumed charge-neutral, so that electro-osmotic flow is absent.<sup>1</sup> Further, local electroneutrality is invoked, which enables us to express the electric field in terms of the instantaneous concentration distributions rather than solve Poisson’s equation for the electric potential. This considerably simplifies the numerical work as Poisson’s equation is stiff due to the smallness of the Debye length. Thus, the problem is reduced to solving a set of one-dimensional coupled partial differential equations for the ion concentration fields.

### A. Model system

We will consider a three-ion system consisting of sample ions, co-ions, and counter-ions. Results will be expressed in terms of dimensionless variables: all lengths are in units of a characteristic length  $w_0$  determined by the initial peak width, time is in units of  $w_0/v$ , where  $v$  is the migration velocity of an isolated sample ion in the applied field ( $E^\infty$ ), and the electric potential is in units of  $E^\infty w_0$ . All concentrations are in units of  $c_n^\infty$ , where  $c_n^\infty$  is the concentration of negative ions in the background electrolyte. In order to define a minimal problem with the fewest possible parameters, we assume that the mobility ( $u$ ) is the same for all the species, and therefore so is the diffusivity ( $D$ ), in accordance with the Einstein relation ( $D_i/u_i = D/u = k_B T$ , where  $k_B$  is Boltzmann’s constant and  $T$  is the absolute temperature). Note, however, that since the valence  $z_i$  are different, the electrophoretic mobilities of the species  $\mu_i = z_i e u$  are not identical. Then the only parameters in the problem are  $Pe = v w_0/D$ , which may be regarded as a “Péclet number” based on the electromigration velocity  $v$ , and the two valence ratios  $z_n/z_p, z_p/z_c$ , where  $z_p, z_n$ , and  $z_c$  are, respectively, the valence of cations, anions, and the sample. We present results for two values of the Péclet number,  $Pe = 100$  and  $200$ , and we fix the valence ratio at  $z : z_p : z_n = 1 : 2 : -1$ . For other values of these parameters, the results are qualitatively similar. The parameter of greatest interest is the degree of sample loading or the amplitude of the initial peak. The shape of the wave is insensitive to initial conditions, so for convenience we take the initial peak shape

to have a rectangular<sup>2</sup> profile of height  $c_m$  and width  $2w_0$  centered at  $x = 10w_0$ . This is also the most common initial shape encountered in practice where the sample is introduced by electrokinetic injection. The degree of sample loading is conveniently characterized [5] in terms of the quantity

$$\Gamma = \int_{-\infty}^{+\infty} \phi(x,t) dx = \int_{-\infty}^{+\infty} \frac{c_n}{c_n^\infty} dx, \quad (1)$$

which has units of length. The length scale  $\Gamma$  may be used to define a second Péclet number  $P = v\Gamma/D$ , which may be treated as a dimensionless measure of sample loading. A series of simulations are conducted with peak heights in the range  $\phi_m = c_m/c_n^\infty = 0.01$  (low sample loading) to  $2.0$  (high sample loading). The initial co-ion concentration  $c_p$  is assumed constant throughout the domain. Then the counter-ion concentration is determined by the local electroneutrality constraint, Eq. (3). An infinite domain is approximated by a finite computational box of length much greater than  $w_0$ . The values of the concentrations are held fixed at the domain boundaries and  $\partial\phi_e/\partial x$  is set to the constant value  $-E^\infty$ . The domain is chosen to be sufficiently large that the perturbations of the concentrations and fields are always negligible near the domain boundaries.

### B. Numerical method

We will solve the governing equations for ion transport in solution, which are

$$\frac{\partial c_i}{\partial t} + \frac{\partial}{\partial x} \left[ -\mu_i c_i \frac{\partial \phi_e}{\partial x} - D_i \frac{\partial c_i}{\partial x} \right] = 0, \quad (2)$$

where  $c_i$  is the concentration of species  $i$  ( $i = 1, 2, \dots, N$ ) with electrophoretic mobility  $\mu_i$  and diffusivity  $D_i$ . Electro-osmotic flow is neglected so that the problem is one-dimensional and may be described using the coordinate  $x$  along the capillary and time since injection,  $t$ . Due to the requirement of local electroneutrality [9],

$$\sum_{i=1}^N z_i c_i = 0 \quad (3)$$

( $z_i$  is the valence of the  $i$ th species). The electric potential  $\phi_e$  may be found from the equation of current conservation:

$$\frac{\partial}{\partial x} \left[ -\sum_{i=1}^N z_i \mu_i c_i \frac{\partial \phi_e}{\partial x} - \sum_{i=1}^N z_i D_i \frac{\partial c_i}{\partial x} \right] = 0. \quad (4)$$

Equation (4) may be readily integrated to yield the local electric field,  $E = -\partial_x \phi_e$ :

$$E(x,t) = \frac{E^\infty \sum_i z_i \mu_i c_i^\infty + \sum_i z_i D_i \partial_x c_i}{\sum_i z_i \mu_i c_i}, \quad (5)$$

where the superscript  $\infty$  indicates the value of the respective variable far away from the peak and the summation is over all species.

A finite volume method is used to discretize Eqs. (2) and (4) in space using an adaptive grid refinement algorithm that is

<sup>1</sup>The effect of a wall zeta potential was recently investigated [16].

<sup>2</sup>To reduce numerical errors, the corners of the rectangle were slightly “rounded” by using a tan hyperbolic function.

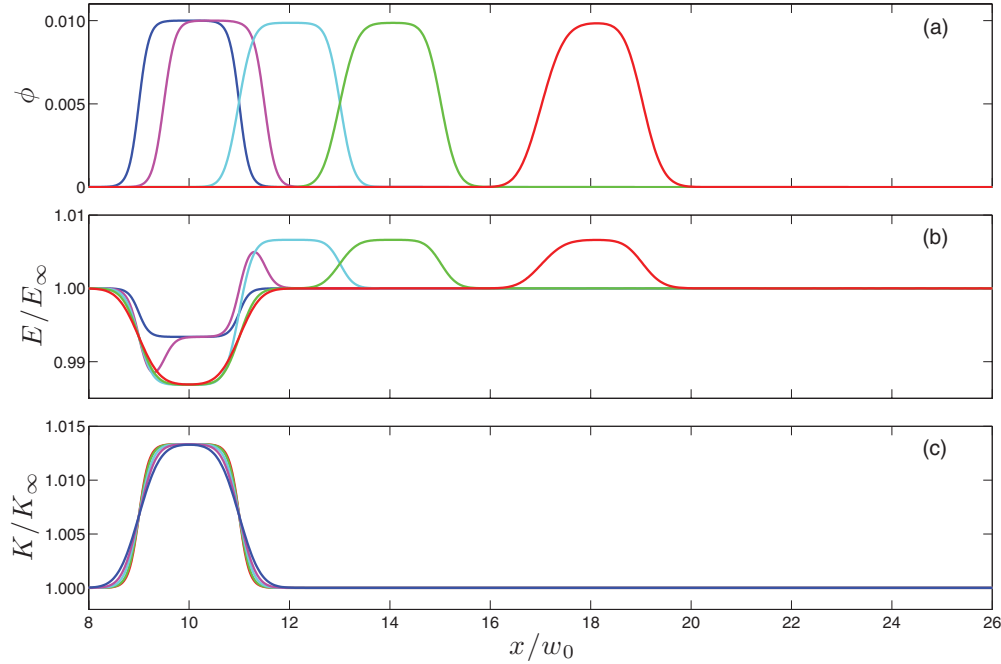


FIG. 1. (Color online) Time evolution of the profiles of the normalized sample ion concentration ( $\phi$ ), electric field ( $E/E_\infty$ ), and Kohlrausch function ( $K/K_\infty$ ) in the case of weak sample loading ( $\phi \ll \phi_c$ ). The Kohlrausch function spreads only by diffusion so that the sample peak rapidly migrates into the zone where  $K = K_\infty$  [18].

enabled by applying the MATLAB library “MATMOL” [10]. The spatially discretized system of equations is then integrated in time using the MATLAB solver “ode45” [11], which is based on an explicit Runge-Kutta (4,5) formula. Equations (2) and (4) automatically ensure that the electroneutrality condition, Eq. (3), is satisfied and this is verified at each time step.

### C. Results

Figure 1(a) shows the profiles of the normalized sample concentration  $\phi(x,t) = c_n/c_n^\infty$  at fixed times  $vt/w_0 = 0, 0.5, 2.0, 4.0,$  and  $8.0$  for the case of low sample loading. Figures 1(b) and 1(c) show, respectively, the profiles of the corresponding electric field  $E(x,t)$  and the Kohlrausch regulating function  $K(x,t) = (c_p + c_n + c)/u$ . The Kohlrausch regulating function is a useful quantity for describing electrokinetic transport. If all ionic species have the same diffusivity,  $K(x,t)$  evolves as a passive scalar [5]. If ionic diffusivities are treated as zero, then  $K(x,t)$  is a conserved quantity [12]. It is seen that  $K(x,t)$  remains localized near the injection zone and spreads only slowly by molecular diffusion. The sample peak, on the other hand, moves to the right, and after a short time the sample peak essentially lies in a zone where  $K = K_\infty$ . This illustrates the behavior postulated earlier that makes possible a simplified description in terms of the one-dimensional nonlinear equation [5]:

$$\frac{\partial \phi}{\partial t} + \frac{\partial}{\partial x} \left( \frac{v\phi}{1 - \alpha\phi} \right) = D \frac{\partial^2 \phi}{\partial x^2}. \quad (6)$$

If  $\phi$  is small, Eq. (6) reduces to Burgers’ equation on Taylor expansion of  $(1 - \alpha\phi)^{-1}$ . In the vicinity of the sample peak, the electric field is functionally related to the normalized sample

concentration;  $E = E_\infty/(1 - \alpha\phi)$ . Here  $\alpha$  is the “velocity slope parameter” introduced in [5].

It may be shown [5] that the requirement of positivity of co- and counter-ion concentrations implies that only sample profiles satisfying the condition  $\phi < \phi_c$ , where  $\phi_c$  is a positive number, may be described by the theory. We will call such profiles “realizable.” The critical concentration,  $\phi_c$ , is given by  $\phi_c = (z_p - z_n)/(z_p - z)$  when  $z < 0$  and  $\phi_c = -[z_n(z_p - z_n)]/[z_p(z - z_n)]$  when  $z > 0$ . When the parameter  $\alpha > 0$ , it may be shown with some simple algebra that  $\phi_c < \phi_c' \equiv \alpha^{-1}$  (see the Appendix), so that the singularity implicit in Eq. (6) when  $\phi = \phi_c'$  is never reached for realizable solutions. Figure 2 shows the behavior of the system for initial conditions that are not realizable. In this situation, a stationary “barrier” develops at a fixed spatial location corresponding to a certain value  $\phi = \phi^{\text{inter}} < \phi_c$ . The sample ions move more or less freely on crossing the barrier but are effectively immobilized on the left of the barrier. This is due to the greatly reduced strength of the electric field in the injection zone where the electrical conductivity is high. This is clearly seen in Fig. 2(b), which shows a sharp reduction in the electric field in the injection zone. Only sample ions near the edge of the zone are able to “leak out” and are carried to the right as an advancing wave. Since part of the sample profile remains quasistationary, the assumption of the constancy of the Kohlrausch function,  $K = K_\infty$ , can no longer be made for nonrealizable concentrations. Thus, Eq. (6), which would have led to unphysical negative concentrations for such nonrealizable profiles, is not applicable until after a sufficient time has evolved so that  $\phi$  is reduced to a value below  $\phi^{\text{inter}}$  throughout the domain.

Figure 3 shows the variation in time of the quantity  $(2D)^{-1}d\sigma^2/dt$  (where  $\sigma^2$  is the peak variance) for a series of different values of the diffusivity and sample loading

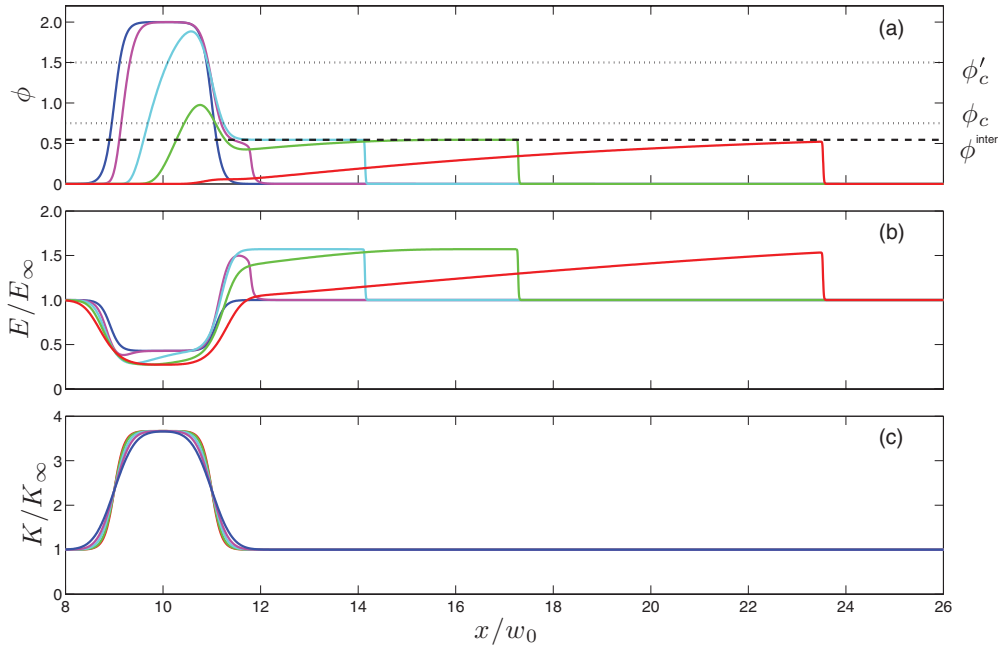


FIG. 2. (Color online) The same as in Fig. 1 except here the amplitude of  $\phi$  exceeds  $\phi_c$ . Here the part of the peak above the value  $\phi = \phi^{\text{inter}}$  appears to be effectively immobilized. The middle panel shows that the stagnant zone is due to a sharp reduction in the electric field caused by the very high electrical conductivity in this zone. The assumption  $K = K_\infty$  is clearly invalid as a part of the peak remains trapped in the injection zone [18].

characterized by the pair of Péclet numbers (Pe,P). If the profile spread purely by molecular diffusivity, this quantity should approach 1 asymptotically. However, it is seen that the long-time asymptotic value is not 1 but rather  $D_{\text{eff}}$ , which depends solely on  $P$ . The dashed line shows the theoretical value of  $D_{\text{eff}}$  predicted by the weakly nonlinear theory based on solutions of Burgers' equation [5]. Thus, once the system has evolved long enough, and dispersion has caused the

amplitude to drop sufficiently, Burgers' equation provides a valid description of the peak evolution. However, a real separation happens in a finite capillary and the long-time limit may not necessarily apply. A quantity of interest is the time scale characterized by  $t_*$ : the time needed for the quantity  $(2D)^{-1}d\sigma^2/dt$  to relax to 0.95 of its asymptotic value  $D_{\text{eff}}$ . If the separation is conducted in a capillary of length  $L$ , the question of interest is whether  $t_*$  is small or large compared to the total separation time  $T = L/v$ . In Fig. 4, we show the

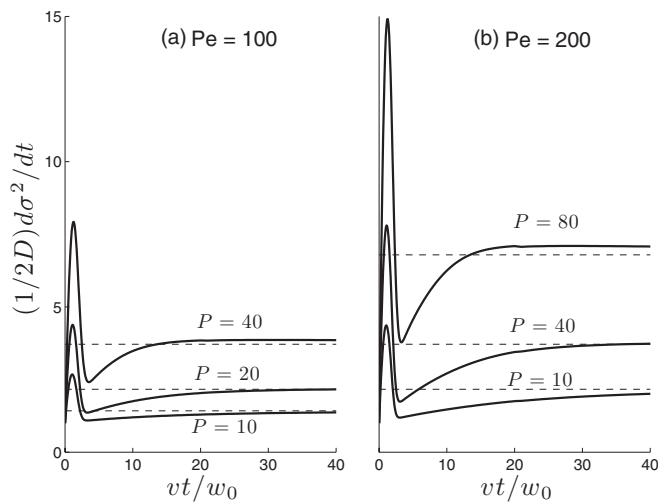


FIG. 3. The normalized rate of change of variance as a function of dimensionless time  $vt/w_0$  for (a)  $Pe = 100$  and (b)  $Pe = 200$  for three different values of sample loading ( $P$ ). At long times, the peak is seen to spread with an effective diffusivity  $D_{\text{eff}} = \lim_{t \rightarrow \infty} (2D)^{-1}(d\sigma^2/dt)$  given by Eq. (37) of [5] and indicated here by the horizontal dashed line.

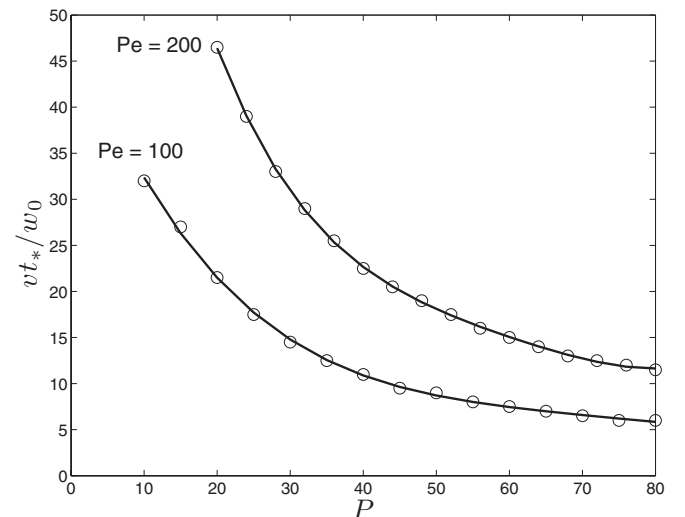


FIG. 4. The normalized convergence time  $vt_*/w_0$ , where  $t_*$  is the time taken for the effective variance  $(2D)^{-1}(d\sigma^2/dt)$  to reach 95% of its final asymptotic value of  $D_{\text{eff}}$  as a function of the sample loading ( $P$ ) for different values of the Péclet number ( $Pe$ ).

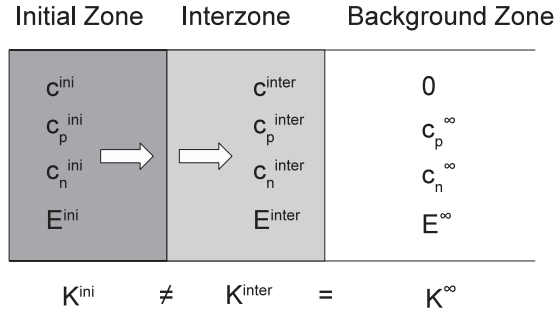


FIG. 5. Schematic diagram describing approximately the initial phase of peak evolution when  $\phi > \phi_c$ . The domain can be divided into an “initial zone,” an “interzone,” and a “background zone.” All the dependent variables are approximately constant within each zone but may undergo jumps across zone boundaries.

normalized time  $vt_*/w_0$  from a series of simulations with different values of  $(\text{Pe}, P)$ . Clearly,  $vt_*/w_0$  is a monotonically decreasing function of  $P$ . This can be anticipated from the theory of nonlinear waves [6]: the higher the amplitude, the quicker a shock or shocklike structure is formed. In contrast to the effective diffusivity shown in Fig. 3, which depends on  $P$  but not on  $\text{Pe}$ , the time to reach the asymptotic state does depend on  $\text{Pe}$ . In fact, as Fig. 4 shows, the curve  $vt_*/w_0$  as a function of  $P$  is shifted upward as  $\text{Pe}$  is increased. Indeed, larger  $\text{Pe}$  corresponds to lower diffusivity and therefore a longer time for the peak to spread and its amplitude to fall sufficiently for the weakly nonlinear description to be valid. Typical values of the physical parameters in a microchip-based system may be  $w_0 \sim 100 \mu\text{m}$ ,  $L \sim 5 \text{cm}$ , so that  $vT/w_0 \sim 500$ . Thus, Fig. 4 suggests that Burgers’ solution does describe the peak dynamics for most of the separation time except for possibly a relatively short initial transient.

#### D. Analysis

An approximate theoretical determination of the concentration  $\phi^{\text{inter}}$  may be provided using the conservation equations. The method of doing this is in fact entirely analogous to the “moving boundary equations” (MBE) [13] for describing advancing fronts (e.g., in isotachopheresis), except, in this case, the front happens to be quasistationary. The conceptual framework is illustrated in Fig. 5. The domain is decomposed into three parts: the “initial zone,” where the sample is injected, the “background zone” ahead of the advancing wave, where all concentrations equal their initial values, and an “interzone” between them. All variables are assumed constant within each zone but undergo a discontinuous change across zone boundaries. The values of the variables in each zone are indicated in Fig. 5. The boundary between the initial zone and the interzone is stationary whereas the boundary between the interzone and the background zone moves to the right. The arrows indicate fluxes of ions across the stationary zone boundary. Conservation of these ionic fluxes requires

$$E^{\text{ini}} \phi^{\text{ini}} = E^{\text{inter}} \phi^{\text{inter}}, \quad (7)$$

$$E^{\text{ini}} \phi_n^{\text{ini}} = E^{\text{inter}} \phi_n^{\text{inter}}, \quad (8)$$

where  $E$  represents the electric field and  $\phi$  represents the concentration (normalized by  $c_n^\infty$ ). The superscript (“ini” for the initial zone, “inter” for the interzone, and “ $\infty$ ” for the background zone) indicates the zone in which the variable is evaluated and the subscript ( $p$  for cation,  $n$  for anion, and no subscript for the sample) identifies the species. Therefore,

$$\phi_n^{\text{inter}} = (\phi_n^{\text{ini}}/\phi^{\text{ini}}) \phi^{\text{inter}}. \quad (9)$$

For the interzone,

$$\begin{aligned} K^{\text{inter}} &= c_n^\infty (\phi^{\text{inter}} + \phi_p^{\text{inter}} + \phi_n^{\text{inter}}) / u \\ &= K_\infty = c_n^\infty (\phi_p^\infty + 1) / u \\ &= c_n^\infty (1 - z_n/z_p) / u. \end{aligned} \quad (10)$$

The electroneutrality condition (valid in all zones) is

$$z_p \phi_p + z_n \phi_n + z \phi = 0. \quad (11)$$

By combining Eqs. (9) and (10) and using the electroneutrality condition, we get an equation for determining  $\phi^{\text{inter}}$ ,

$$(1 - z/z_p) \phi^{\text{inter}} + r(1 - z_n/z_p) \phi^{\text{inter}} = 1 - z_n/z_p, \quad (12)$$

where the ratio  $\phi_n^{\text{ini}}/\phi^{\text{ini}} = r$  is a constant determined by the ionic composition of the injected zone. Solving the above linear equation for  $\phi^{\text{inter}}$ , we have

$$\phi^{\text{inter}} = [r + (z_p - z)/(z_p - z_n)]^{-1}. \quad (13)$$

In our numerical experiment, the cation concentration was chosen to be uniform, so that  $\phi_p^{\text{ini}} = \phi_p^\infty = -z_n/z_p$ . Since  $z : z_p : z_n = 1 : 2 : -1$ ,  $r = 1/\phi_p^{\text{ini}} - z/z_n = 1.5$  and  $\phi^{\text{inter}} = 0.55$ . This value is indicated by the dashed line in Fig. 2(a). Clearly, it correctly describes the concentration of sample in the interzone.

Thus, the theoretical description developed in [5] may be used in the interzone ( $\phi < \phi^{\text{inter}}$ ) but not in the initial zone. In order for all ion concentrations to be non-negative in the interzone, we must have  $\phi^{\text{inter}} < \phi_c < \phi'_c$ . This inequality is indeed true, as can be shown by some simple algebra (see the Appendix).

### III. CONCLUSIONS

The development of nonlinear waves in capillary electrophoresis in the limit of a low as well as a high concentration of sample ions was studied by numerical integration of the governing equations. An idealized minimal model was considered consisting of a three-ion (sample, co-ion, and counter-ion) system of strong electrolytes.<sup>3</sup> This study complements an earlier paper by the authors. There it was shown that, in the weakly nonlinear limit, the evolution of the sample concentration may be reduced to Burgers’ equation, which admits an exact analytical solution.

Numerical simulation revealed that the evolution of the peak proceeds in a way that is qualitatively different when the sample concentration is high. As a consequence of the sharp reduction of the electric field in the region of sample injection, the ion migration velocity in this zone is very small. Ahead of

<sup>3</sup>The situation of a weak electrolytic buffer was recently investigated by the authors [17].

this zone, the ions form a surge front with a steplike profile propagating to the right. This state of affairs continues until the dimensionless ion concentration ( $\phi$ ) in the injection zone drops sufficiently so that  $\phi < \phi^{\text{inter}}$ . The subsequent dynamics then proceeds in accordance with the weakly nonlinear theory [5]. The value of  $\phi^{\text{inter}}$  may be approximately calculated by using a simple model based on conservation of ionic fluxes.

This qualitative change in the dynamics of peak evolution explains the breakdown of the weakly nonlinear theory when the concentration  $\phi$  exceeds the critical value  $\phi_c$ . When  $\phi$  exceeds a certain value  $\phi^{\text{inter}} < \phi_c$ , part of the propagating wave is effectively immobilized in the injection zone. It is then no longer correct to assume [5] that the sample pulse would quickly move out to a region where the Kohlrausch function is constant.

The model studied here is clearly oversimplified. In particular, real electrophoresis buffers contain many more than three ions, including one or more weak acids or bases to maintain a stable pH. Further, complex effects due to inhomogeneities in the electro-osmotic flow may be relevant [14]. In this paper, we ignore these complexities and attempt to produce a detailed understanding of a “minimal” model problem. One may question whether the strongly nonlinear regime considered here is of relevance to actual laboratory practice. The answer depends on the numerical values of the critical concentrations  $\phi^{\text{inter}} < \phi_c < \phi'_c$ . If the sample and carrier ions have similar valences, then all of these critical concentrations are of order unity. Thus, to exceed these critical values, the sample ions in the injected plug will need to be present at concentrations approaching that of the carrier electrolyte. Such high concentrations are rarely employed in laboratory practice. However, if the sample is a macro-ion, the critical values may actually be quite small. For example, at pH 2.0, bovine serum albumin has a valence,  $z \sim 55$  [15]. Then, in a univalent carrier electrolyte, we have  $\phi_c \sim 0.04$ , so that the strongly nonlinear regime studied here may be easily reached.

**ACKNOWLEDGMENTS**

This work was supported by the National Institute of Health under Grant No. R01EB007596.

**APPENDIX: PROOF OF THE INEQUALITY  $\phi^{\text{inter}} < \phi_c < \phi'_c$**

The critical concentration  $\phi_c$  is defined as [5]

$$\phi_c = \begin{cases} \frac{z_p - z_n}{z_p - z} & \text{if } z < 0, \\ -\frac{z_n}{z_p} \frac{z_p - z_n}{z - z_n} & \text{if } z > 0, \end{cases} \quad (\text{A1})$$

whereas

$$\phi'_c = \frac{1}{\alpha} = \frac{z_n(z_p - z_n)}{(z - z_n)(z - z_p)}. \quad (\text{A2})$$

We need to show that  $\phi_c < \phi'_c$  when  $\alpha > 0$ , that is, when  $z_p > z > z_n$ . To do this, evaluate the ratio  $\phi_c/\phi'_c$  when  $z_p > z > z_n$ :

$$\frac{\phi_c}{\phi'_c} = \begin{cases} \frac{z_p - z_n}{z_p - z} \frac{(z - z_n)(z - z_p)}{z_n(z_p - z_n)} = \frac{-z_n + z}{-z_n} < 1 & \text{if } z < 0, \\ -\frac{z_n}{z_p} \frac{z_p - z_n}{z - z_n} \frac{(z - z_n)(z - z_p)}{z_n(z_p - z_n)} = \frac{z_p - z}{z_p} < 1 & \text{if } z > 0, \end{cases} \quad (\text{A3})$$

which completes the proof.

To prove the remaining inequality,  $\phi^{\text{inter}} < \phi_c$ , we first show that  $r > -z/z_n$  when  $z < 0$ . To do this, we use the electroneutrality condition to express  $\phi_p^{\text{ini}}$  in terms of the other variables,

$$\phi_p^{\text{ini}} = -\frac{z}{z_p} \phi^{\text{ini}} - \frac{z_n}{z_p} \phi_n^{\text{ini}} = \frac{\phi^{\text{ini}}}{z_p} (-z - r z_n). \quad (\text{A4})$$

Now we must have  $\phi_p^{\text{ini}} > 0$ . This is always true if  $z < 0$ , but if  $z > 0$ , then we require that  $r > -z/z_n$ .

First suppose that  $z < 0$ . Then

$$\begin{aligned} \phi^{\text{inter}} &= \frac{1}{r + (z_p - z)/(z_p - z_n)} \\ &< \frac{1}{(z_p - z)/(z_p - z_n)} = \frac{z_p - z_n}{z_p - z} = \phi_c. \end{aligned} \quad (\text{A5})$$

Now suppose that  $z > 0$ . Then

$$\begin{aligned} \phi^{\text{inter}} &= \frac{1}{r + (z_p - z)/(z_p - z_n)} \\ &< \frac{1}{-(z/z_n) + (z_p - z)/(z_p - z_n)} \\ &= -\frac{z_n}{z_p} \frac{z_p - z_n}{z - z_n} = \phi_c. \end{aligned} \quad (\text{A6})$$

Thus, in all cases,  $\phi^{\text{inter}} < \phi_c$ , which completes the proof.

---

[1] *Handbook of Capillary Electrophoresis*, edited by J. Landers (CRC, Boca Raton, FL, 1996).  
 [2] *Capillary Electrophoresis, Theory & Practice*, edited by P. Camilleri (CRC, Boca Raton, FL, 1998).  
 [3] S. Ghosal, *Annu. Rev. Fluid Mech.* **38**, 309 (2006).  
 [4] J. Jorgenson and K. Lukacs, *Anal. Chem.* **53**, 1298 (1981).  
 [5] S. Ghosal and Z. Chen, *Bull. Math. Biol.* **72**, 2047 (2010).  
 [6] G. Whitham, *Linear and Nonlinear Waves* (Wiley-Interscience, New York, 1974).  
 [7] F. Mikkers, F. Everaerts, and T. P. Verheggen, *J. Chromatogr.* **169**, 1 (1979).  
 [8] J. J. Stoker, *Commun. Pure Appl. Math.* **1**, 1 (1948).  
 [9] I. Rubinstein, *Electro-Diffusion of Ions* (SIAM, Philadelphia, 1990).  
 [10] A. Vande Wouwer, P. Saucez, and W. E. Schiesser, *Ind. Eng. Chem. Res.* **43**, 3469 (2004).  
 [11] L. F. Shampine and M. W. Reichelt, *SIAM J. Sci. Comput.* **18**, 1 (1997).  
 [12] F. Kohlrausch, *Ann. Phys.* **62**, 209 (1897).  
 [13] V. P. Dole, *J. Am. Chem. Soc.* **67**, 1119 (1945).  
 [14] L. Chen and A. T. Conlisk, *Biomed. Microdev.* **11**, 251 (2008).  
 [15] C. L. Ford and D. J. Winzor, *Biochim. Biophys. Acta: Protein Struct. Molec. Enzymol.* **703**, 109 (1982).  
 [16] S. Ghosal and Z. Chen, *J. Fluid Mech.* **697**, 436 (2012).  
 [17] Z. Chen and S. Ghosal, *Bull. Math. Biol.* **74**, 346 (2012).  
 [18] See supplemental material at <http://link.aps.org/supplemental/10.1103/PhysRevE.85.051918> for a movie of the time evolution depicted in Figs. 1 and 2.